The Mechanism of Phosphodiester Hydrolysis: Near In-line Attack Conformations in the Hammerhead Ribozyme

Rhonda A. Torres and Thomas C. Bruice*

Contribution from the Department of Chemistry, University of California, Santa Barbara, California 93106

Received August 25, 1999

Abstract: The hammerhead ribozyme is a small RNA molecule capable of self-cleavage at a specific site in the phosphodiester backbone. The mechanism of hydrolysis involves in-line nucleophilic attack by the 2′-hydroxyl of residue 17 on the adjoining phosphorus of residue 1.1, resulting in the formation of a 2′,3′-cyclic phosphate ester on residue 17 (C_{17}) and elimination of the 5′-hydroxyl group of residue 1.1 ($A_{1.1}$). *Unconstrained* molecular dynamics (MD) simulations on the recently solved crystallographic unmodified hammerhead ribozyme structure were performed in solution using two crystallographic Mg^{2+} ions. The simulations indicate that near in-line attack conformations (NACs), in which the distance of the 2′-oxygen of C_{17} to the phosphorus of $A_{1.1}$ is ≤3.25 Å and the C_{17} 2′O−$A_{1.1}$ P−$A_{1.1}$ O5′ angle of displacement is ≥150°, form approximately 18% of the simulation time. The motions leading to these catalytically competent conformations are discussed. Stems I and II of the hammerhead ribozyme structure, released from the pseudo-continuous helix and other crystallographic constraints, move toward each other. This, along with the Mg^{2+} ion bound at the *pro-R* phosphate oxygen of residue 1.1, prompts torsional rotations in the phosphodiester backbone primarily near the active site. These rotations lead to the unstacking of residues C_{17} and G_5 from A_6. Residue G_5 then interacts with other conserved residues in the structure and does not stack with A_6 again. Following spontaneous backbone conformational rearrangements, a ribose sugar pucker flip from C3′-*endo* to C2′-*endo* occurs in the nucleotide containing the 2′-hydroxyl nucleophile. The base of residue C_{17} then restacks with the base of residue A_6, and NACs occur shortly thereafter. During the simulations, one Mg^{2+} ion remains coordinated to the *pro-R* phosphate oxygen of the C_{17} nucleotide, while the other Mg^{2+} ion serves a structural role and does not participate in the transesterification reaction. The formation of NACs is spontaneous during the simulation and in a replicate simulation.

Introduction

The hammerhead ribozyme (Scheme 1) is a self-catalytic RNA hydrolase comprised of a conserved, single-stranded catalytic core region of 15 nucleotides (in outlined letters)[1] surrounded by three Watson−Crick base-paired stems.[2−4] Site-directed mutagenesis experiments on this consensus sequence[5] have identified modifications that drastically affect the rate of cleavage.[4,6−8] The hammerhead ribozyme typically utilized for *in vitro* studies is separated into two strands, with one strand functioning as the enzyme (E) and the other as the substrate (S). The strands assemble due to base pairing interactions in the three stems. The hammerhead, thus, cleaves *in trans* and is capable of multiple turnovers, with typical cleavage rates of 1 min^{-1}.[2,9]

The two plausible mechanisms for nucleophilic displacement at phosphate phosphorus [$S_N2(P)$] involve in-line and adjacent attack geometries (Scheme 2). The in-line mechanism involves nucleophile approach to phosphorus at an angle of 180° relative to the leaving oxygen with inversion of configuration about the phosphorus. In the adjacent attack geometry, the nucleophile approaches the phosphorus at an angle of 90° to the leaving oxygen and the pentacovalent intermediate must pseudorotate so that the departing oxygen leaves from an apical position.[10] The configuration about the phosphorus is inverted during self-cleavage of the hammerhead ribozyme.[8,11,12] These and other experimental studies[13−15] show that in-line displacement is the clear course of nucleophilic attack in hammerhead and enzymatic systems. Adjacent attack is made most difficult due to the steric requirements of pseudorotation on the structure of the catalyst. The $S_N2(P)$ mechanism for the hammerhead transesterification involves the 2′-oxygen of residue C_{17} in an in-line displacement of the 5′-leaving group of the adjoining nucleotide to give a 2′,3′-cyclic phosphate ester and a 5′-hydroxyl (Scheme 3).[5,16] The log of the cleavage rate was shown to increase linearly with pH between 5.7 and 8.9 with a slope

* To whom correspondence should be addressed. E-mail: tcbruice@bioorganic.ucsb.edu.

(1) Hertel, K. J.; Pardi, A.; Uhlenbeck, O. C.; Koizumi, M.; Ohtsuka, E.; Uesugi, S.; Cedergren, R.; Eckstein, F.; Gerlach, W. L.; Hodgson, R.; Symons, R. H. *Nucleic Acids Res.* **1992**, *20*, 3252.
(2) Uhlenbeck, O. C. *Nature* **1987**, *328*, 596−600.
(3) Symons, R. H. *Annu. Rev. Biochem.* **1992**, *61*, 641−71.
(4) Ruffner, D. E.; Stormo, G. D.; Uhlenbeck, O. C. *Biochemistry* **1990**, *29*, 10695−10702.
(5) Buzayan, J. M.; Gerlach, W. L.; Bruening, G. *Proc. Natl. Acad. Sci. U.S.A.* **1986**, *83*, 8859−8862.
(6) Fu, D.-J.; McLaughlin, L. W. *Biochemistry* **1992**, *31*, 10941−10949.
(7) McKay, D. B. *RNA* **1996**, *2*, 395−403.
(8) Slim, G.; Gait, M. J. *Nucleic Acids Res.* **1991**, *19*, 1183−1188.
(9) Fedor, M. J.; Uhlenbeck, O. C. *Biochemistry* **1992**, *31*, 12042−12054.
(10) Westheimer, F. H. *Acc. Chem. Res.* **1968**, *1*, 70−78.
(11) van Tol, H.; Buzayan, J. M.; Feldstein, P. A.; Eckstein, F.; Bruening, G. *Nucleic Acids Res.* **1990**, *18*, 1971−1975.
(12) Koizumi, M.; Ohtsuka, E. *Biochemistry* **1991**, *30*, 5145−5150.
(13) Usher, D. A.; Richardson, D. I.; Eckstein, F. *Nature* **1970**, *228*, 663−665.
(14) Usher, D. A. *Proc. Natl. Acad. Sci. U.S.A.* **1969**, *62*, 661−667.
(15) Usher, D. A.; Erenrich, E. S.; Eckstein, F. *Proc. Natl. Acad. Sci. U.S.A.* **1972**, *69*, 115−118.
(16) Hutchins, C. J.; Rathjen, P. D.; Forster, A. C.; Symons, R. H. *Nucleic Acids Res.* **1986**, *14*, 3627−3640.

10.1021/ja993094p CCC: $19.00
Published on Web 01/19/2000

Scheme 1

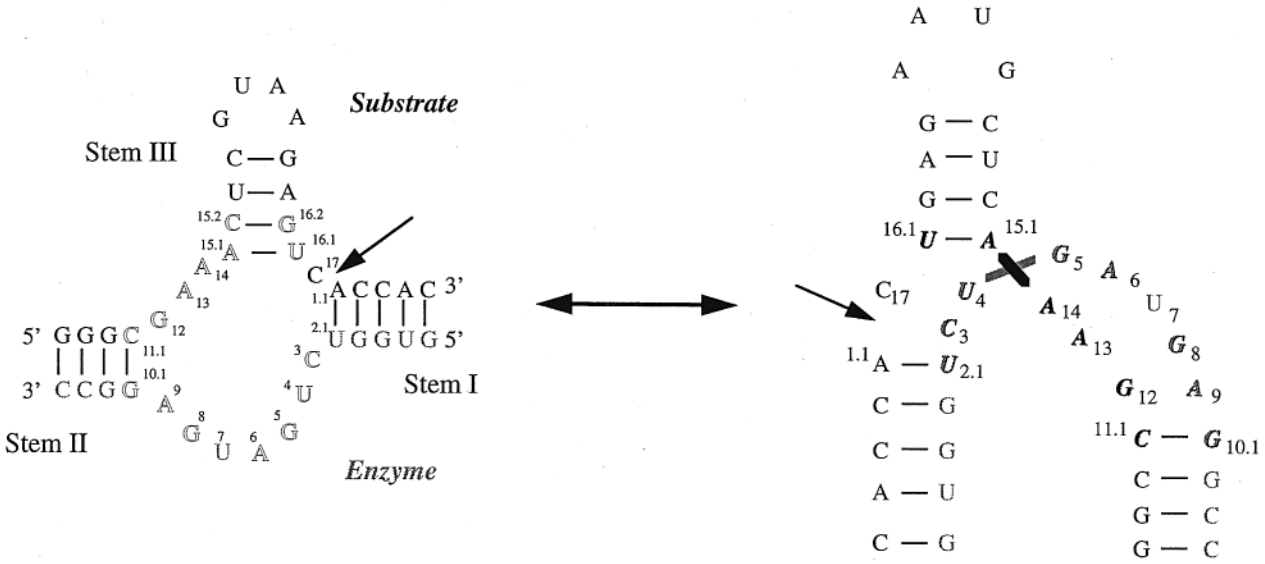

Scheme 2

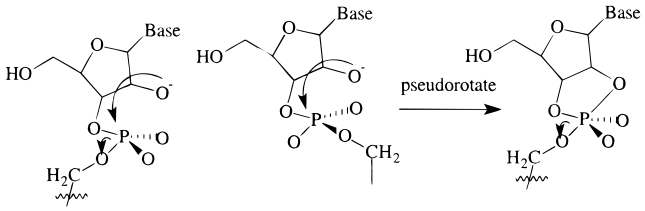

In-line Attack (no pseudorotation) **Adjacent Attack** (pseudorotation required)

of unity, indicating a specific base or kinetically equivalent deprotonation of the 2′-hydroxyl group.[8,17,18] Two kinetically equivalent mechanisms of in-line nucleophilic attack can be considered (Scheme 4). One involves a metal-ligated hydroxide, acting as a general base, by removing the proton of 2′-OH at residue C_{17}. The second possible mechanism is that of specific base catalysis, where a lyate HO^- brings about the ionization of the 2′-OH nucleophile with the metal ion participating elsewhere in the reaction. It has been shown experimentally that a metal ion ligates to the *pro-*R_P oxygen of the $-O-(PO_2^-)-O-$ moiety undergoing reaction. This feature is paramount to metal ion catalysis of nucleophilic hydrolysis of phosphodiesters.[8,12,19−22] In this way, the negative charge on the phosphate moiety is neutralized, and nucleophilic attack upon the phosphate is facilitated. This divalent metal ion, or perhaps another, can perform the necessary stabilization of the 5′-leaving group. This could be accomplished by orienting a water molecule such that a proton may be donated to the leaving group or via direct interaction of the metal ion with the leaving group oxygen.

Recently, several crystal structures of the hammerhead ribozyme have been solved.[23−26] The unmodified hammerhead crystal structures solved at low pH in the presence and absence of divalent metal ions are quite similar to each other and a crystal structure containing a 2′-O-methyl modification at residue C_{17},[25] with a heavy atom rms deviation of 0.5 Å. These structures depict the attacking 2′-hydroxyl in an orientation consistent with an unprecedented adjacent attack. It is important to determine the hammerhead conformation(s) that allow an in-line displacement reaction.

The 3.0 Å crystal structure of an unmodified hammerhead ribozyme, solved by flash freezing at pH 8.5 after infusion of a solution of $MgCl_2$ prior to catalysis,[26] is the only unmodified structure containing an assigned Mg^{2+} ion bound to the *pro-R* oxygen of residue $A_{1.1}$ which has been solved thus far. Conformational changes with an rms deviation of approximately 2.9 Å from an identical molecule (solved at the same resolution, without Mg^{2+} ions and at pH 6) were centered at residues C_{17} and $A_{1.1}$. These changes likely resulted from the binding of the Mg^{2+} ion to the *pro-R* oxygen of the scissile phosphate. Further structural rearrangement is seen in the 5′-C-methyl-ribose derivative of residue $A_{1.1}$, in which the nucleobase of C_{17} moves more than 8.7 Å and the scissile phosphate adopts an altered helical geometry from the A-type helical conformation prior to catalysis. None of these structures are in a conformation consistent with the accepted mechanism for RNA hydrolysis. Thus, the conformational changes resulting in reactive ground-state structures remain elusive.

Several groups have carried out computational analysis in the hope of discovering the nature of the structural rearrangements leading to the formation of reactive ground states.[27−31] The earliest computational study on the hammerhead ribozyme

(17) Dahm, S. C.; Derrick, W. B.; Uhlenbeck, O. C. *Biochemistry* **1993**, *32*, 13040−13045.
(18) Dahm, S. A.; Uhlenbeck, O. C. *Biochemistry* **1991**, *30*, 9464−9469.
(19) Blaskó, A.; Bruice, T. C. *Acc. Chem. Res.* **1999**, *32*, 475−484.
(20) Bruice, T. C.; Tsubouchi, A.; Dempcy, R. O.; Olson, L. P. *J. Am. Chem. Soc.* **1996**, *116*, 9867−9875.
(21) Dempcy, R. O.; Bruice, T. C. *J. Am. Chem. Soc.* **1994**, *116*, 4511−4512.
(22) Vanhommerig, S. A. M.; Sluyterman, L. A. Æ.; Meijer, E. M. *Biochim. Biophys. Acta-Protein Struct. Mol. Enzymol.* **1996**, *1295*, 125−138.
(23) Murray, J. B.; Terwey, D. P.; Maloney, L.; Kerpelsky, A.; Usman, N.; Beigelman, L.; Scott, W. G. *Cell* **1998**, *92*, 665−673.
(24) Pley, H. W.; Flaherty, K. M.; McKay, D. B. *Nature* **1994**, *372*, 68−74.
(25) Scott, W. G.; Finch, J. T.; Klug, A. *Cell* **1995**, *81*, 991−1002.
(26) Scott, W. G.; Murray, J. B.; Arnold, J. R. P.; Stoddard, B. L.; Klug, A. *Science* **1996**, *274*, 2065−2069.
(27) Mei, H. Y.; Kaaret, T. W.; Bruice, T. C. *Proc. Natl. Acad. Sci. U.S.A.* **1989**, *86*, 9727−9731.
(28) Torres, R. A.; Bruice, T. C. *Proc. Natl. Acad. Sci. U.S.A.* **1998**, *95*, 11077−11082.
(29) Setlik, R. F.; Shibata, M.; Sarma, R. H.; Sarma, M. H.; Kazim, A. L.; Ornstein, R. L.; Tomasi, T. B.; Rein, R. *J. Biomol. Struct. Dyn.* **1995**, *13*, 515−522.

Scheme 3

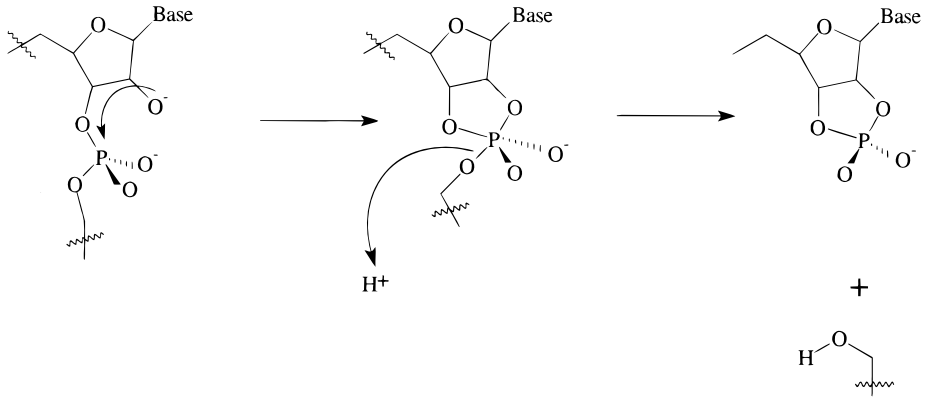

Scheme 4

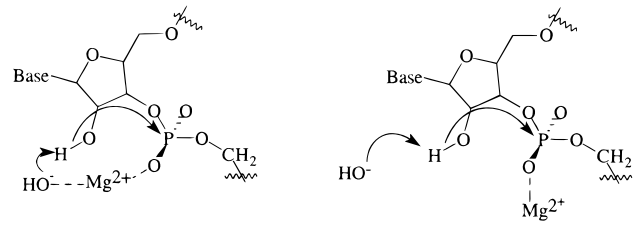

General Base **Specific Base**

predicted that the unpaired nucleotide containing the internal nucleophile (residue C_{17}) rotates out toward solution (effect **A**).[27] It was also suggested in this study that effect **A** was likely accompanied by a C3′-*endo* to C2′-*endo* ribose sugar repuckering in this residue (effect **B**), such that in-line attack conformations would then occur. A more recent study utilized the all-RNA ribozyme structure with a 2′-O-methyl modification[25] at residue C_{17}. It was observed that, following rotations of the phosphodiester backbone at the cleavage site consistent with effect **A**, spontaneous conformational rearrangements leading to reactive conformations of the hammerhead ribozyme were generated. This study also provided insight into the potential roles of conserved core residues in the structural rearrangements related to attaining these reactive conformations.[28] Although insightful, this study did not utilize crystallographic Mg^{2+} ions; the two Mg^{2+} cations were placed consistent with experimental data,[20,21,26] one ligated to the *pro-R* oxygen of residue $A_{1.1}$ and the other as given for site 3.

Here, we report molecular dynamics studies of the unmodified hammerhead ribozyme structure solved at pH 8.5 by Scott and co-workers,[26] incorporating two crystallographic Mg^{2+} ions. In this simulation, we find spontaneous formation of reactive or near in-line attack conformations. The potential roles of many of the conserved core residues are revealed, and details of the structural rearrangements, involving effects **A** and **B**, that lead to near in-line attack conformations in this hammerhead ribozyme are provided.

Theoretical Methods

The 3.0 Å resolution crystal structure (Brookhaven Protein Database refcode: 301d) containing the freeze-trapped, conformational intermediate of the hammerhead ribozyme solved by Scott et al.[26] was used as the starting structure in this molecular dynamics study. Hydrogen atoms were added to the crystal structure. Two magnesium ions from the structure were included: that of site 3 and the Mg^{2+} ion coordinated to the *pro-R* phosphate oxygen of the leaving nucleotide, site 6.[26] The use of two metal ions were deemed appropriate as each metal ion in the structure solved by Scott and co-workers was modeled with an occupancy of 0.5 (see ref 26 for further experimental details). The parameters for the Mg^{2+} ions were taken from Åqvist.[32] Sodium counterions were placed adjacent to the phosphate groups to obtain a system with neutral charge. The ribozyme and associated ions were placed in a cubic box constructed in the EDIT module of AMBER4.1[33] along with approximately 6100 explicit TIP3P[34] water molecules to give the simulation system.

Energy minimization, consisting of 500 steps of steepest descents followed by 9500 steps of conjugate gradient, was performed on the system utilizing the AMBER 5[33] force field. To slowly relax the starting system, the following molecular dynamics protocol was utilized.[28] The constant-volume system was heated to 300 K within the first 20 ps. The constant-volume dynamics were continued for an additional 20 ps, followed by 60 ps of constant-temperature/pressure dynamics using the Berendsen temperature coupling algorithm and periodic boundary conditions. A 10 Å residue-based cutoff was used for the nonbonded interactions. The equilibration portion of the simulation was complete by 100 ps. Following equilibration, production dynamics were conducted using the particle mesh Ewald[35−38] summation method to calculate the electrostatic interactions, with a charge grid spacing of approximately 1 Å. The SHAKE[39] algorithm was used to constrain bonds containing hydrogen. A 1 fs time step was used with a geometric tolerance of 10^{-7} for coordinate resetting. As the B-factors in the active-site region for the RNA are ∼71 Å^2,[26] suggesting that this is region is highly dynamic, no positional restraints were placed on any atoms in the system. This simulation was run for 1.1 ns. A replicate simulation was conducted, also for 1.1 ns, in which the initial seed value for the random number generator used to assign initial velocities was changed. For a conformation to be considered a near attack conformation (NAC), it must meet the following criteria: the angle formed by C_{17} 2′O−$A_{1.1}$ P−$A_{1.1}$ O5′ must be ≥150°, and the distance between C_{17} 2′O−$A_{1.1}$ P must be ≤3.25 Å.[28] The results were analyzed with the CARNAL module of AMBER 5. Visualization and graphical representation of molecular dynamics snapshots were made with MidasPlus.[40,41] The

(30) Hermann, T.; Auffinger, P.; Westhof, E. *Eur. Biophys. J.* **1998**, *27*, 153−165.
(31) Hermann, T.; Auffinger, P.; Scott, W. G.; Westhof, E. *Nucleic Acids Res.* **1997**, *25*, 3421−3427.
(32) Åqvist, J. *J. Phys. Chem.* **1990**, *94*, 8021−8024.
(33) Pearlman, D. A.; Case, D. A.; Caldwell, J. W.; Ross, W. S.; Cheatham, T. E., III.; Ferguson, D. M.; Seibel, G. L.; Singh, U. C.; Weiner, P. K.; Kollman, P. A. *AMBER 4.1*, 5th ed.; University of California: San Francisco, 1995.
(34) Jorgensen, W. L.; Chandrasekhar, J.; Madura, J. D. *J. Chem. Phys.* **1983**, *79*, 926−935.
(35) Cheatham, T. E., III.; Miller, J. L.; Fox, T.; Darden, T. A.; Kollman, P. A. *J. Am. Chem. Soc.* **1995**, *117*, 4193−4194.
(36) Essmann, U.; Perera, L.; Berkowitz, M. L.; Darden, T. A.; Lee, H.; Pedersen, L. G. *J. Chem. Phys.* **1995**, *103*, 8577−8593.
(37) Darden, T. A.; York, D.; Pedersen, L. G. *J. Chem. Phys.* **1993**, *98*, 10089−10092.
(38) Chen, Z. M.; Çagin, T.; Goddard, W. A., III. *J. Comput. Chem.* **1997**, *18*, 1365−1370.
(39) van Gunsteren, W. F.; Berendsen, H. J. C. *Mol. Phys.* **1977**, *34*, 1311−1327.

average distance and angle data were calculated for the production dynamics period only.

Results and Discussion

The starting crystal structure of the hammerhead ribozyme for molecular dynamics simulations contained two Mg^{2+} ions. Two Mg^{2+} ions are believed to be required for the proper folding of the catalytically active hammerhead ribozyme.[42,43] The first ion, corresponding to site 3, is located in the region known as domain 2, which consists of residues U_7, G_8, A_9, G_{12}, A_{13}, and A_{14}; and the second, corresponding to site 6, is located in the active site, or domain I, which consists of residues C_3, U_4, G_5, A_6, C_{17}, and $A_{1.1}$. Many of the structural rearrangements leading to reactive conformations in this study are similar to those seen in our previous MD study which were based on the structure of the 2′-O-methyl modified hammerhead.[28]

Structural Changes at Active Site Preceding First Set of Reactive Near Attack Conformations (NACs). During molecular dynamics simulations, it was observed that the global conformation or relative orientation of the stems in the hammerhead ribozyme was retained; however, substantial changes from the starting crystal structure were observed. Many of these changes relate to the utilization of a single hammerhead ribozyme molecule, thus removing the pseudo-continuous helix stacking found in the asymmetric crystal. As a consequence of removing these and other crystal lattice restraints, stems I and II begin to tilt toward each other. This motion has been observed in other dynamics simulations on the hammerhead ribozyme[28−31] and is believed to be necessary for catalysis.[7] Stems I and II were also found to be in close proximity in the crystal structure of the RNA−DNA hammerhead ribozyme construct.[24]

The Mg^{2+} ion at site 3 in domain 2 moves quickly from this original position to associate with the *pro-S* oxygen of residue G_8 where it remains for the duration of the simulation time, with an average distance of 1.96 ± 0.04 Å. The positioning of this divalent cation serves a critical structural role in the hammerhead and helps to stabilize the sharp turn between Stem I and Stem II. Thus, it appears unlikely that this metal ion directly participates in the mechanism of catalysis.

The active site for this ribozyme consists of domain I, or the uridine turn, and the two residues bordering in the scissile phosphate bond, C_{17} and $A_{1.1}$. This site also contains the Mg^{2+} ion bound to the *pro-R* phosphate oxygen of residue $A_{1.1}$ in the starting structure. Phosphorothioate modifications of this oxygen have resulted in a loss of activity when the metal ion is Mg^{2+}.[4,8,12] Thus, the binding of a metal ion to this oxygen has been implicated in the cleavage mechanism. Binding of a Mg^{2+} ion to this oxygen appears to induce the structural rearrangements in the hammerhead ribozyme that lead to reactive conformations.[42−46] This can also be seen when the crystal structures solved by Scott and co-workers are compared.[26] Taken together, the experimental data suggest that binding of Mg^{2+} to the *pro-R* phosphate oxygen of residue $A_{1.1}$ induces conformational changes in the backbone of both strands and orients nucleotides at the active site to generate reactive conformations. The Mg^{2+} ion undoubtedly functions as a Lewis acid catalyst by neutralizing the negative charge on the scissile phosphate.

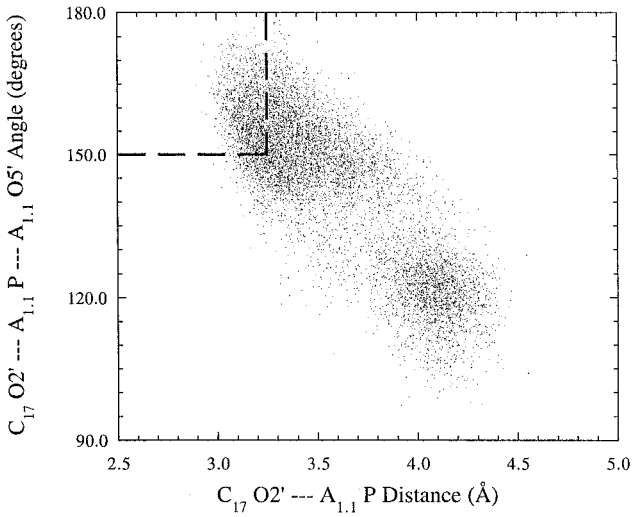

Figure 1. Plot of the angle vs distance approach of the 2′-hydroxyl of residue C_{17} to the phosphate of residue $A_{1.1}$ for the first simulation. Near in-line attack conformations (NACs) for this simulation are located in the box defined by a distance ≤3.25 Å between the 2′-oxygen of C_{17} to the phosphorus of $A_{1.1}$ and an angle ≥150° for the displacement of the leaving group (O5′) of residue $A_{1.1}$. The cluster of points near 3.3 Å and 150° corresponds to the ribose of C_{17} in the C2′-*endo* conformation, while the cluster of points centered around 4.1 Å and 120° correspond to this ribose ring in the C3′-*endo* conformation.

The phosphate backbone in the substrate strand of the active site begins to rotate (effect **A**) during energy minimization. The stacking platform of G_5, A_6, and C_{17}, found in the starting crystal structure, is disrupted by these backbone rotations. The Mg^{2+} ion remains coordinated to the *pro-R* oxygen, with an average distance of 1.95 ± 0.04 Å, and thus moves as the phosphate group moves during the simulation. Initially, the remaining inner sphere coordination sites of this Mg^{2+} are occupied by water molecules. One water molecule is displaced from the inner coordination sphere of this Mg^{2+}, and the N7 of $A_{1.1}$ occupies its position. The N7 of purine bases is known to directly coordinate to Mg^{2+}.[47] Next, another inner sphere water molecule departs, and this coordination site becomes occupied by the O6 of $G_{2.2}$. Once the N7 and O6 coordinate to the Mg^{2+}, they remain coordinated for the rest of the dynamics run, as do water molecules wat4057 and wat4110. The average coordination distance for the N7 of $A_{1.1}$ and the O6 of $G_{2.2}$ to the catalytic Mg^{2+} are 2.25 ± 0.09 and 2.04 ± 0.06 Å, respectively. Although residues $A_{1.1}$ and $G_{2.2}$ are nonconserved residues in the hammerhead ribozyme, it has been shown that the innermost base pairs in stem I participate in the cleavage reaction and the fastest rate is achieved when these two positions were occupied by uridine.[48] The change in rate may be due to the fact that disruption of a U-A Watson−Crick base pair is easier than disrupting a G-C base pair and the uridine would provide an oxygen ligand to the Mg^{2+} ion. Following unstacking of residue G_5 from the G_5-A_6-C_{17} platform (discussed below), a spontaneous sugar pucker flip occurs from C3′-*endo* to C2′-*endo* in residue C_{17} (effect **B**), and the bases of A_6 and C_{17} restack with one another. A water molecule, wat638, migrates into the active

(40) Huang, C. C.; Pettersen, E. F.; Klein, T. E.; Ferrin, T. E.; Landridge, R. *J. Mol. Graphics* **1991**, *9*, 230−236.
(41) Ferrin, T. E.; Huang, C. C.; Jarvis, L. E.; Landridge, R. *J. Mol. Graphics* **1988**, *6*, 13−27.
(42) Amiri, K. M. A.; Hagerman, P. J. *J. Mol. Biol.* **1996**, *261*, 125−134.
(43) Bassi, G. S.; Murchie, A. I. H.; Walter, F.; Clegg, R. M.; Lilley, D. M. J. *EMBO J.* **1997**, *16*, 7481−7489.
(44) Wedekind, J. E.; McKay, D. B. *Annu. Rev. Biophys. Biomol. Struct.* **1998**, *27*, 475−502.
(45) Peracchi, A. *Nucleic Acids Res.* **1999**, *27*, 2875−2882.
(46) Bassi, G. S.; Møllegaard, N. E.; Murchie, A. I. H.; Lilley, D. M. J. *Biochemistry* **1999**, *38*, 3345−3354.
(47) Cowan, J. A. *The Biological Chemistry of Magnesium*; VCH Publishers: New York, 1995; p 254.
(48) Clouet-d'Orval, B.; Uhlenbeck, O. C. *Biochemistry* **1997**, *36*, 9087−9092.

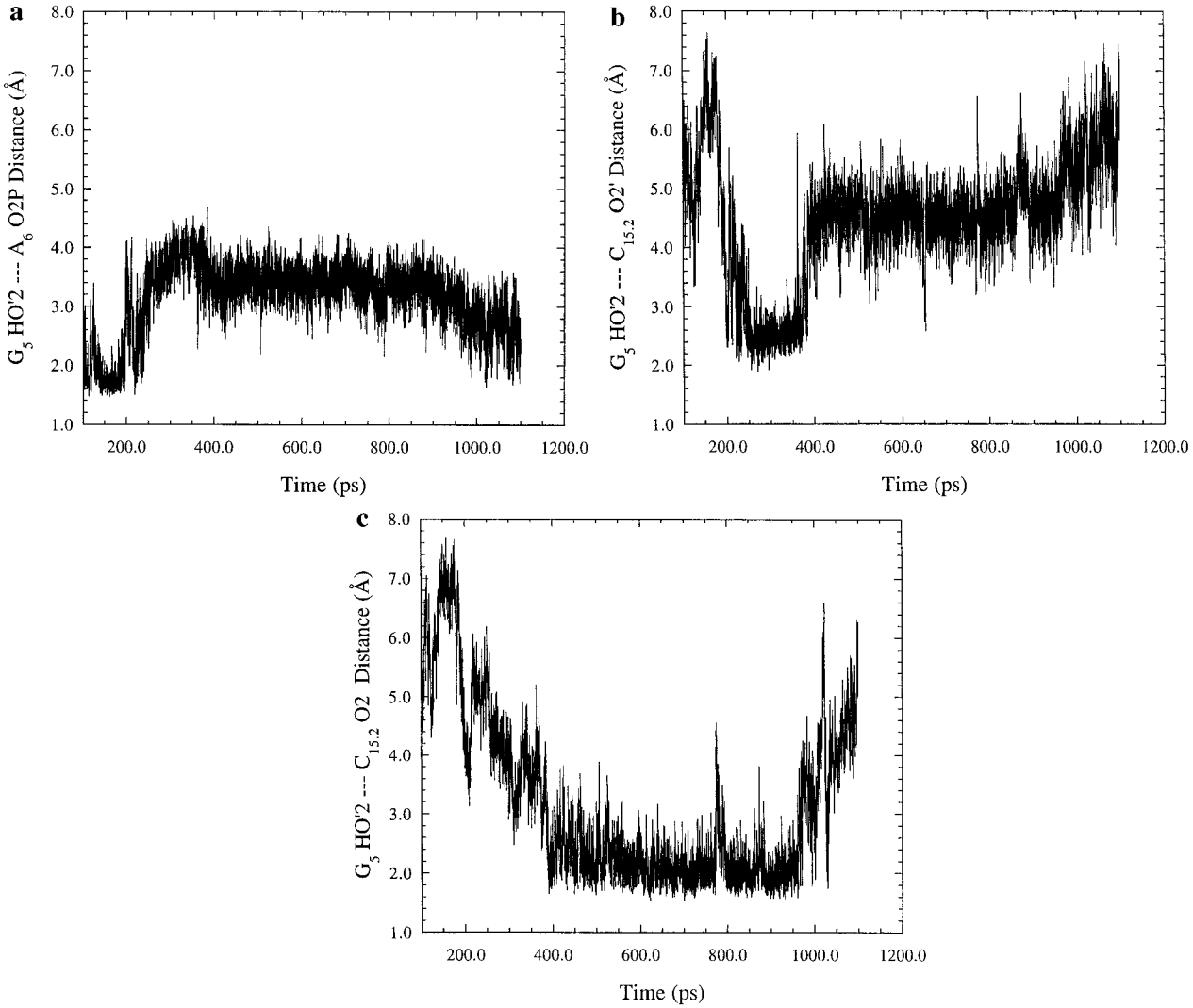

Figure 2. Interactions of the 2′-hydroxyl of residue G_5 with residues A_6 and $C_{15.2}$. (a) Following the equilibration period, a tight hydrogen bond forms between the hydrogen of the 2′-hydroxyl of G_5 and the *pro-R* oxygen of A_6. This hydrogen bond persists until a sugar pucker flip to the C3′-*endo* conformation occurs in residue C_{17}. (b) A hydrogen bond between the 2′-hydroxyl groups of residues G_5 and $C_{15.2}$ forms during the period of time (200−400 ps) when the sugar pucker of residue C_{17} is in the C3′-*endo* conformation. (c) Following the sugar pucker flip back to the C2′-*endo* conformation in C_{17} at approximately 400 ps, a hydrogen bond forms between the 2′-hydroxyl of G_5 and the O2 atom in the base of residue $C_{15.2}$.

Chart 1

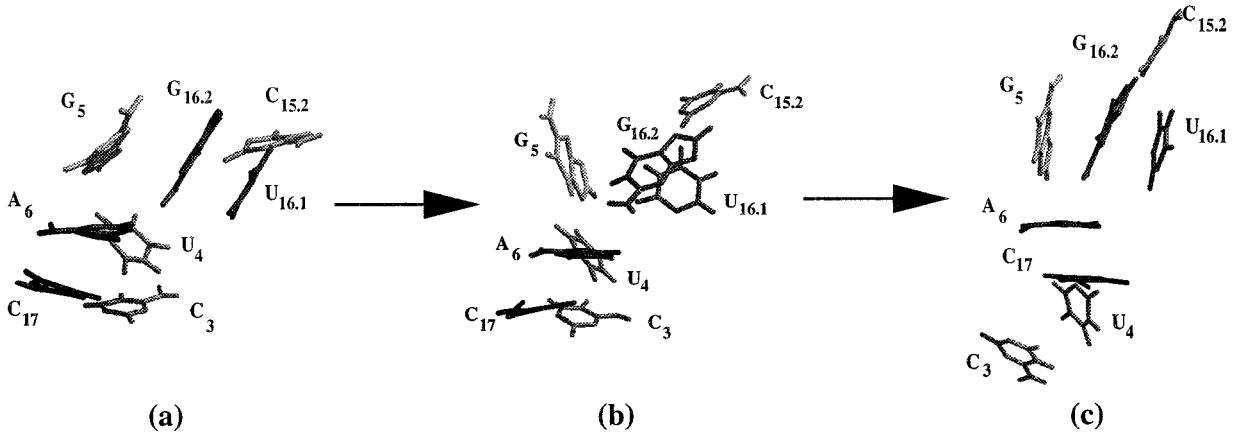

site just prior to the sugar pucker flip in residue C_{17} and coordinates to the Mg^{2+}. Once wat638 becomes ligated, it remains coordinated to this Mg^{2+} ion. Near in-line attack conformations (NACs) are then spontaneously generated. NACs are those structures in which the distance of the O2′ of the internal nucleophile to the phosphorus undergoing the displacement reaction is ≤3.25 Å with an angle of displacement ≥150°. NACs are observed approximately 18% of the simulation time (Figure 1) and begin forming shortly after 100 ps of total simulation time.

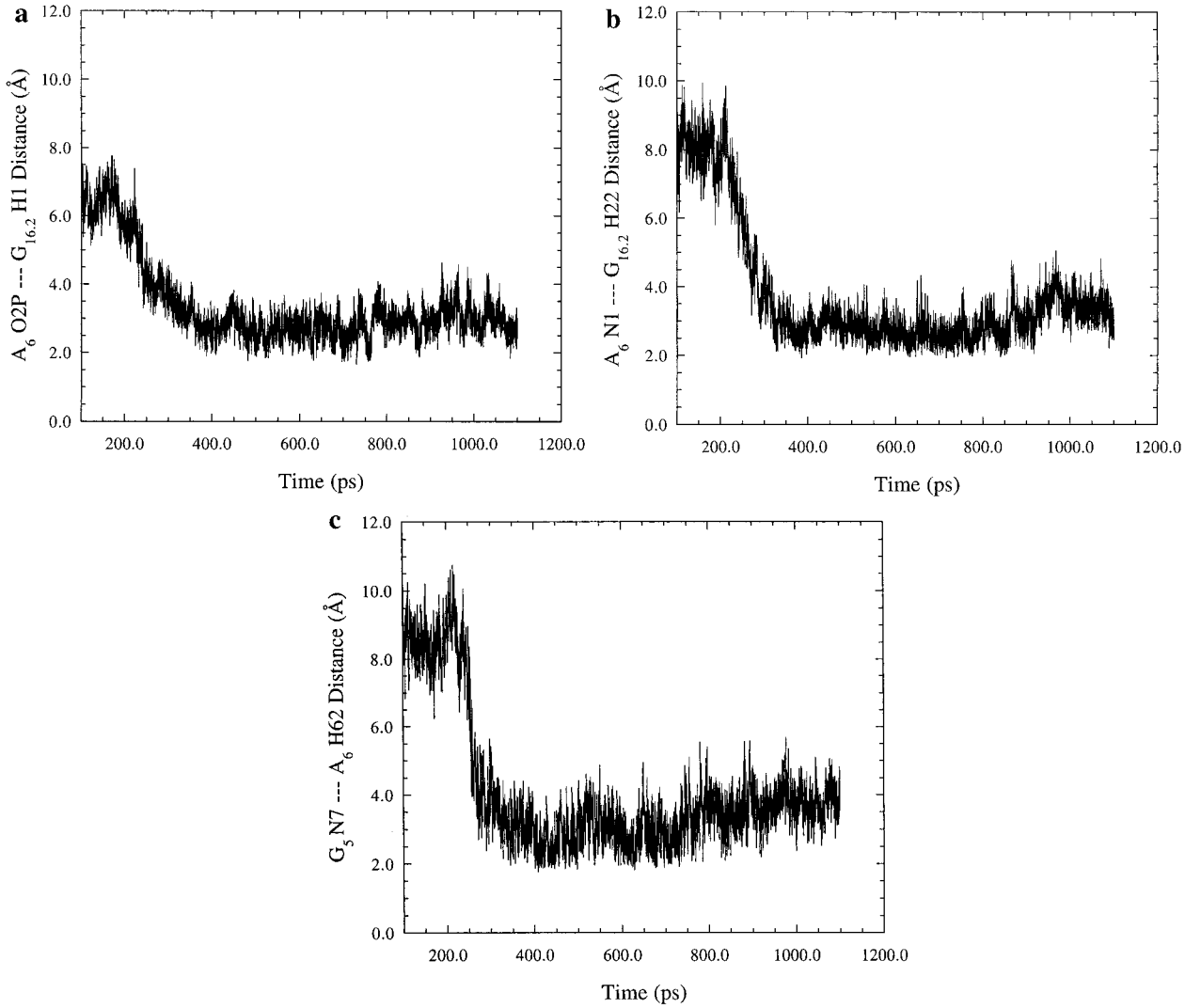

Figure 3. (a) Histogram of the hydrogen bond that forms between the *pro-R* oxygen of residue A_6 and the H1 of residue $G_{16.2}$ following the sugar pucker flip in residue C_{17}. (b) Due to the proximity of residues A_6 and $G_{16.2}$ following the formation of the hydrogen bond in (a), the hydrogen bond between the N1 of A_6 and H22 of $G_{16.2}$ develops. (c) The restacking of residue G_5 and the sugar pucker flip to the C3′-*endo* conformation in residue C_{17} results in the formation of a hydrogen bond between the N7 of G_5 and H62 of residue A_6.

Residue G_5 undergoes large motions during the simulation. The motions of G_5 and other nearby nucleotides are summarized in Chart 1. In the equilibration portion of the dynamics, a hydrogen bond between the 2′-hydroxyl of G_5 and the O2 of residue $C_{15.2}$ formed, but was quickly broken in favor of hydrogen bonds between the 2′-hydroxyl groups of G_5 and $C_{15.2}$. During the backbone rotations at the active site in the substrate strand, a sugar pucker flip to C2′-*endo* occurs in residue $U_{16.1}$. This results in base stacking of $U_{16.1}$ with the base of residue $G_{16.2}$. After residue G_5 unstacks from the G_5-A_6-C_{17} platform, it rotates around and stacks with the platform formed by residues $G_{16.2}$ and $U_{16.1}$ until the sugar pucker of residue C_{17} flips to the C2′-*endo* conformation (Chart 1a). The G_5-$G_{16.2}$-$U_{16.1}$ platform is temporarily disrupted. While residues $G_{16.2}$ and $U_{16.1}$ reform the platform, the base of G_5 is exposed to solvent, and there appear to be no substantial interactions of the base with any other base in the ribozyme, except for a hydrogen bond that forms between the N7 of G_5 and the H1 of residue $G_{16.2}$ (Chart 1b). The hydrogen bond between the 2′-hydroxyls of G_5 and $C_{15.2}$ breaks toward the end of the equilibration period and the 2′-hydroxyl of G_5 forms a hydrogen bond with the *pro-R* phosphate oxygen of residue A_6 (Figure 2, Chart 2a). The aforementioned sugar pucker flip to the C3′-*endo* conformation

Chart 2

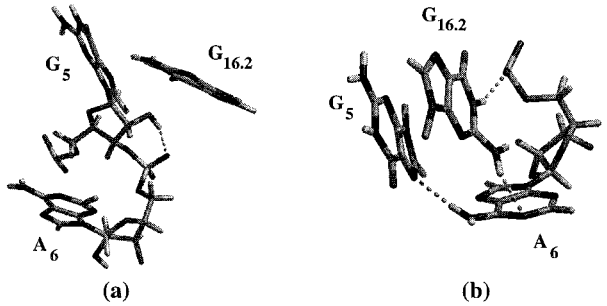

occurs in residue C_{17}, and near in-line attack conformations (NACs) are then generated.

The base of residue G_5 slowly rotates such that it restacks with the $G_{16.2}$-$U_{16.1}$ platform (Chart 1c). During this rotation, the hydrogen bond to the *pro-R* oxygen of A_6 breaks at approximately 200 ps of total simulation time, as seen in Figure 2a. This oxygen then forms a persistent hydrogen bond with the H1 of residue $G_{16.2}$ (Figure 3a). Due to the proximity of A_6 and $G_{16.2}$ at this point, a hydrogen bond forms between the N1 of A_6 and the exocyclic amine of $G_{16.2}$ (Figure 3b). The loss of the hydrogen bond to the *pro-R* oxygen of A_6 coincides with

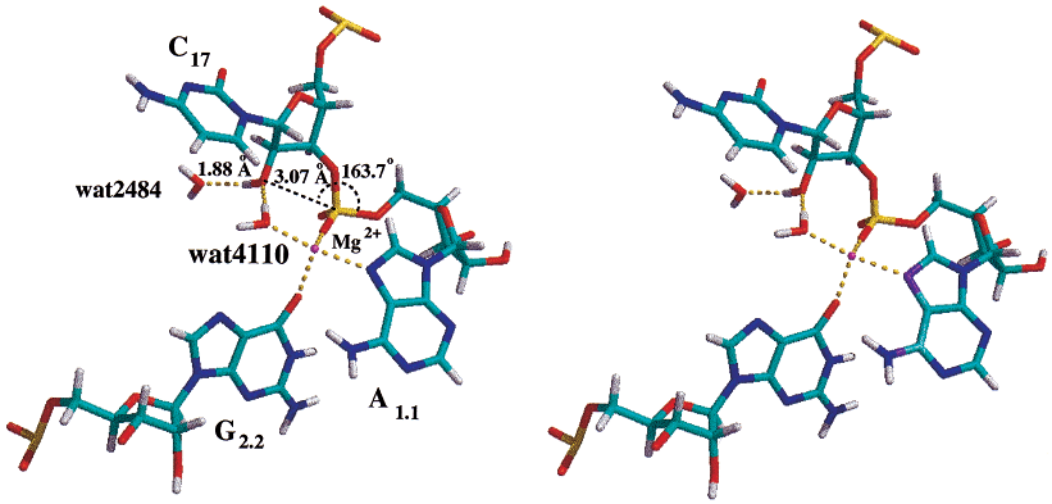

Figure 4. Snapshot of the active site displaying a near in-line attack conformation (NAC) of mechanistic importance. A water molecule, wat2484, has moved into the active site and hydrogen bonds to the hydrogen of the 2′-hydroxyl of residue C_{17}; the hydrogen bonding distance is 1.88 Å. The hydrogen bonding distance between an inner sphere, Mg^{2+}-coordinated water molecule wat4110 is 1.77 Å. Here, the attack distance and the angle of displacement are 3.07 Å and 163.7°, respectively. The remaining Mg^{2+} coordination sites are occupied by two water molecules (wat638 and wat4057) which are not shown for clarity.

the sugar pucker flip in residue C_{17} to the C3′-*endo* conformation. However, it is not known if the breaking of this hydrogen bond is related to this sugar pucker flip. The hydrogen bond between the N7 of G_5 and H1 of residue $G_{16.2}$ also breaks following the sugar pucker flip in C_{17}, and a new hydrogen bond forms between the N7 of G_5 and the exocyclic amine of A_6, as seen in Chart 2b and Figure 3c. The 2′-hydroxyl of G_5 then forms a persistent hydrogen bond with the O2 of $C_{15.2}$ for approximately 600 ps when it breaks to reform the hydrogen bond with the *pro-R* oxygen of residue A_6 (Figure 2a). It appears that the alternating hydrogen bonds between the 2′-hydroxyl of G_5 and residues $G_{16.2}$ and A_6 work in concert to form reactive conformations, which may explain the 10^3 fold decrease in activity when the 2′-hydroxyl is absent.[6,49,50] Due to the large degree of motions the base of residue G_5 undergoes and the apparent lack of interactions with other conserved bases prior to the generation of NACs, it appears that mutations of G_5 likely impedes proper folding[43,46] and the formation of reactive conformations.

Features Consistent with Mechanism of Hydrolysis. Following the restacking of G_5 with the $G_{16.2}$-$U_{16.1}$ platform and the sugar pucker flip to C2′-*endo* in residue C_{17}, an inner sphere water molecule of the catalytic Mg^{2+} (wat4110) forms a hydrogen bond to the ribose 2′-oxygen of C_{17} as a water molecule (wat2484) moves into the active site. The oxygen of wat2484 then hydrogen bonds to the hydrogen of the 2′-hydroxyl of residue C_{17}. Hydrogen bonds between these water molecules and the nucleophilic 2′-hydroxyl occurs during the formation of NACs (Figure 4). Wat2484 moves more than 30 Å from its starting position and remains in the active site for a short period of time (∼10−15 ps) and then it leaves while NACs are still forming. As the hydrogen bond between the 2′-hydroxyl of C_{17} and the oxygen of wat2484 breaks and this water begins to move out of the active site, the Mg^{2+} ion moves closer to the O5′ of residue $A_{1.1}$ and oscillates between ∼4.35 and 3.66 Å from the leaving oxygen (Figure 5). The coordination about the Mg^{2+} remains the same. The attack distance slowly lengthens, and the attack angle becomes smaller until the conformations are

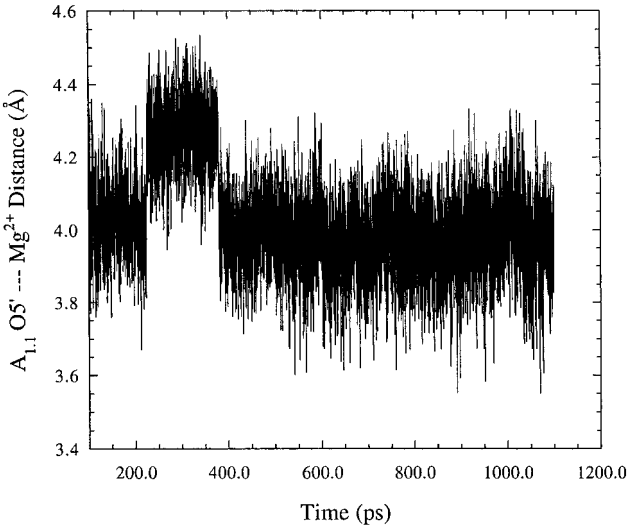

Figure 5. Plot of the distance between the catalytic Mg^{2+} ion (bound to the *pro-R* oxygen in the active site) and the O5′ of residue $A_{1.1}$. The average distance between these two atoms is 4.03 ± 0.15 Å.

no longer NACs. Indeed, NACs do not occur when the distances between this Mg^{2+} and the leaving group oxygen are less than 3.8 Å. This distance lengthens to approximately 4.4−4.6 Å when the Mg^{2+} moves away slightly to return to the average distance of 4.03 ± 0.15 Å. The catalytic metal ion does not ligate to the internal nucleophile, as evidenced by the average distance of 4.98 ± 0.61 Å between the Mg^{2+} and the 2′-oxygen of residue C_{17} during the simulation. As wat638 and wat2484 (and later wat5237, see below) migrate into the active site, the simulation is in accord with either free HO^- or metal bound HO^- ionizing the 2′-hydroxyl to generate the nucleophile in the mechanism of metal cation mediated hydrolysis.

NACs Do Not Form When the Ribose Conformation of C_{17} is C3′-*endo*. A spontaneous sugar pucker flip from C2′-*endo* to C3′-*endo* in residue C_{17} resulted after wat2484 departed from the active site, and NACs are not formed between 200 and 400 ps. The C2′-*endo* conformation is spontaneously restored, and NACs re-occur. NACs are formed consistently during production dynamics except when the sugar pucker of residue C_{17} is in the C3′-*endo* conformation. The base stacking

(49) Tuschl, T.; Ng, M. M. P.; Pieken, W.; Benseler, F.; Eckstein, F. *Biochemistry* **1993**, *32*, 11658−11668.
(50) Williams, D. M.; Pieken, W. A.; Eckstein, F. *Proc. Natl. Acad. Sci. U.S.A.* **1992**, *89*, 918−921.

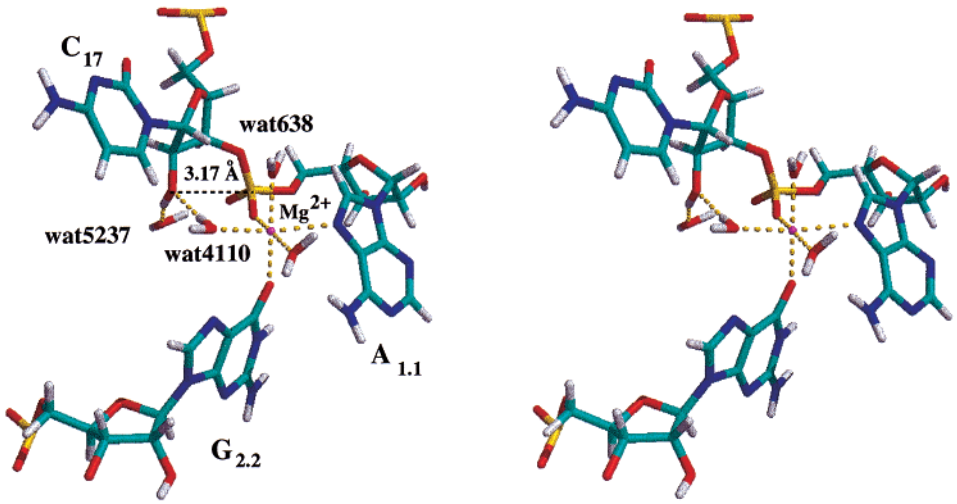

Figure 6. Enlarged view of the active site of a NAC in which the oxygen of wat5237 has migrated into the active site to hydrogen bond with the 2′-hydroxyl of the attacking nucleophile on residue C_{17}. The distance between the oxygen of wat5237 and the hydrogen on the 2′-hydroxyl is 1.68 Å. Wat4110, an inner sphere water molecule ligated to the Mg^{2+} cation, is also hydrogen bonded to the 2′-oxygen with a distance of 1.95 Å. The distance and angle for attack on the phosphorus of residue $A_{1.1}$ is 3.17 Å and 172.7°, respectively. Wat5237 remains close to the 2′-hydroxyl for approximately 25 ps before it departs from the active site.

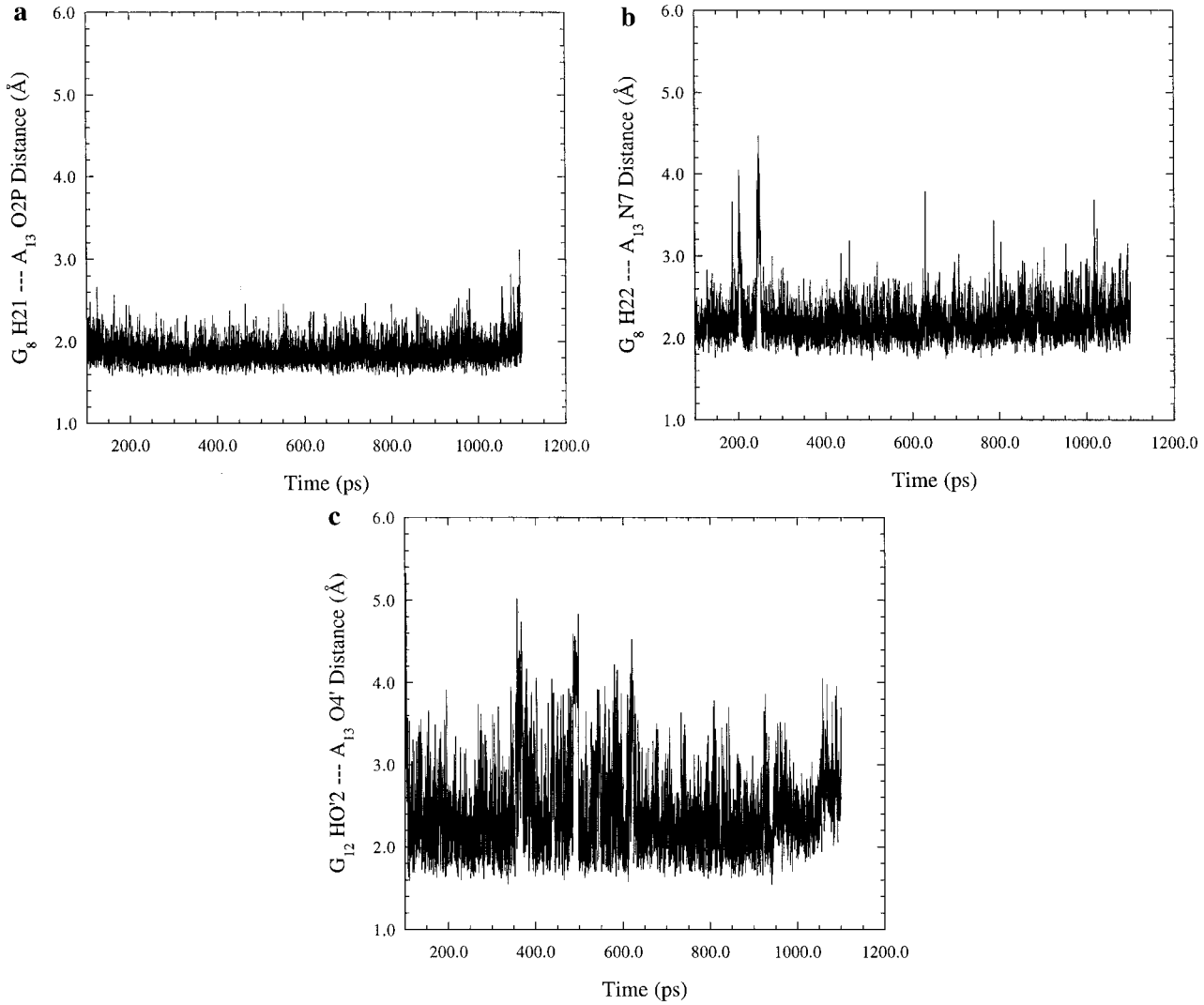

Figure 7. Plots of interactions of residue A_{13} with residues G_8 and G_{12} during production dynamics. (a) A hydrogen bond forms early between one of the exocyclic amine hydrogens (H21) of G_8 and the *pro-R* oxygen of residue A_{13}. The average distance of this hydrogen bond is 1.86 ± 0.13 Å. (b) Presumably as a result of the proximity of A_{13} and G_8 due to the hydrogen bond formed in (a), a hydrogen bond forms between the N7 of A_{13} and the other exocyclic amine hydrogen (H22) of G_8 with an average distance of 2.22 ± 0.25 Å. (c) A hydrogen bond was observed between the 2′-hydroxyl of residue G_{12} and the O4′ of A_{13} (average distance is 2.41 ± 0.51 Å). These hydrogen bonds, along with the base stacking between G_{12} and A_{13} serves to help maintain the proper orientation of the backbone in this region of the hammerhead.

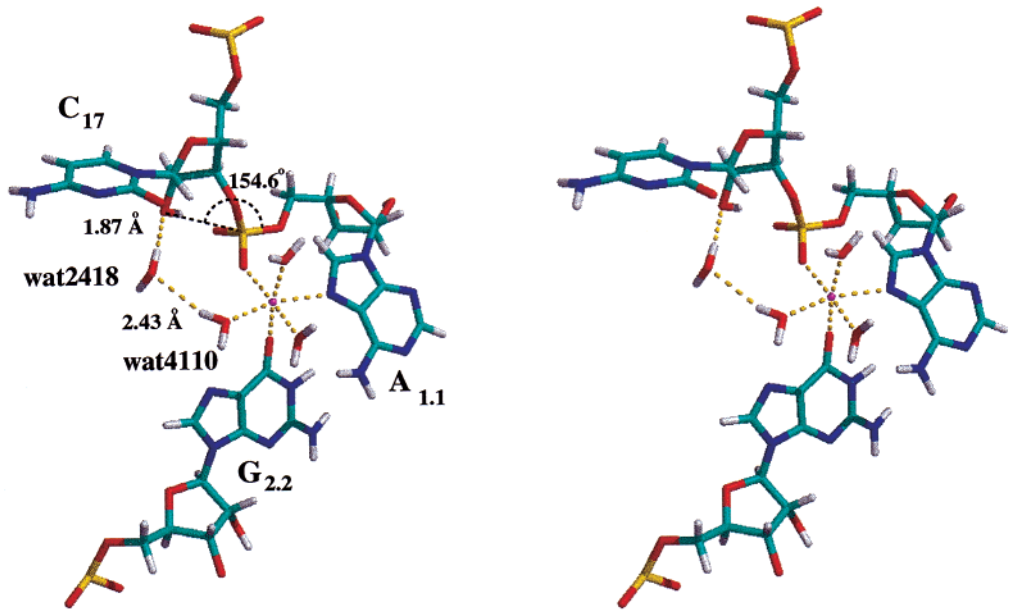

Figure 8. Snapshot of the active site during a near attack conformation in the replicate simulation. Wat2418 has migrated into the active site to hydrogen bond with the 2′-oxygen of residue C_{17} with a distance of 1.87 Å. The oxygen of wat2418 also hydrogen bonds to the hydrogen of an inner sphere coordinated water molecule, wat4110, with a distance of 2.43 Å. The other Mg^{2+} ion coordination sites are occupied by the *pro-R* oxygen and N7 of residue $A_{1.1}$, the O6 of residue $G_{2.2}$, and the oxygen atoms of wat4057 and wat4345; the distances between these atoms and the Mg^{2+} ion are 1.98, 2.29, 2.11, 2.12, and 2.02 Å, respectively. Wat4345 migrated into the active site and ligated to the Mg^{2+} ion following the sugar pucker flip from C3′-*endo* to C2′-*endo* in residue C_{17} and prior to the formation of NACs. The attack distance in this NAC is 3.15 Å with an attack angle of 154.6°.

platform of G_5-$G_{16.2}$-$U_{16.1}$ is maintained as is the base stacking between $A_{1.1}$ and C_{17}. Following the ribose pucker flip back to the C2′-*endo* conformation, a second set of NACs occurs after 500 ps. A second water molecule, wat5237, also migrates into the active site and forms a hydrogen bond with the 2′-hydroxyl of residue C_{17} (Figure 6). This water molecule remains in the active site for about 20−25 ps, and then it departs from the active site. The same type of movement of the catalytic Mg^{2+} ion toward the departing oxygen is seen following the departure of wat2484, although the range incorporates lower values, from 4.35 to 3.55 Å. There was no sugar pucker flip back to the C3′-*endo* conformation in residue C_{17} prior to the end of the simulation time.

Additional Conserved Core Residue Interactions. During the simulation, it was observed that many favorable interactions occurred between the conserved residues in the hammerhead ribozyme core. These interactions appear to be necessary to properly orient the molecule such that reactive conformations can be generated. Early in the simulation, persistent hydrogen bonds formed between residues A_{13} and G_8. Phosphorothioate modification of the *pro-R* oxygen of A_{13} results in a complete lack of activity of this ribozyme,[4] suggesting that this oxygen participates in binding a metal cation or in a persistent hydrogen bonding interaction. The hydrogen bond between the *pro-R* oxygen of A_{13} and the H21 of the exocyclic amine of G_8 had an average distance of 1.86 ± 0.13 Å (Figure 7a). The average hydrogen bonding distance between the remaining hydrogen of the exocyclic amine of G_8 (H22) and the N7 of residue A_{13} was 2.22 ± 0.25 Å (Figure 7b). Excision of the N7 of residue A_{13} has been shown to result in a decrease in the rate of hydrolysis in the hammerhead ribozyme as have mutations of residue G_8.[6,51] A hydrogen bond also forms between the 2′-hydroxyl of G_{12} and the O4′ of A_{13} with an average distance of 2.41 ± 0.51 Å, as seen in Figure 7c. The base of G_{12} stacks below the base of A_{13}, and this stacking arrangement is maintained for the duration of the simulation.

Following stacking of the G_5 base with the $G_{16.2}$-$U_{16.1}$ platform (Chart 1), a hydrogen bond forms between the O6 of G_{12} and the H22 of $G_{10.1}$ (average distance = 2.85 ± 1.82 Å). These hydrogen bonds along with the stacking of G_8 below A_{12}, serve to orient the strands while G_{12} slowly rotates to stack with the top of Stem II and the bottom of the A_{12}-G_8 platform. Due to further structural rearrangements, this hydrogen bond breaks, and new hydrogen bonds form between the 2′-hydroxyl group of G_8 and H3, O6, and H21 in turn from residue G_{12} as G_{12} slowly rotates in to stack with the top of Stem II (data not shown). These interactions between the conserved core residues assist in orienting the strands such that NACs can spontaneously and repeatedly be generated throughout the simulation.

Replicate Simulation. A replicate simulation was performed utilizing the same minimized starting structure but with a different seed value for the random number generator that assigns the initial velocities for the atoms. In the replicate simulation, 7.3% of the structures represented NACs over the simulation. The average coordination distances of the Mg^{2+} ions to their respective oxygen atoms were identical to the first simulation. The Mg^{2+} ion at site 3 moved quickly to ligate to the *pro*-S oxygen of residue G_8. The average coordination distance between these atoms was 1.96 ± 0.04 Å. The Mg^{2+} ion at site 6, which is bound to the *pro-R* oxygen of the scissile phosphate, remained coordinated throughout the simulation with an average distance of 1.95 ± 0.04 Å. The coordination of the N7 of residue $A_{1.1}$ and the O6 of residue $G_{2.2}$ to the Mg^{2+} ion at the active site were also observed with nearly identical coordination distances when compared to those of the first simulation, 2.24 ± 0.89 and 2.04 ± 0.06 Å, respectively. During the equilibration portion of the replicate simulation, a spontaneous sugar pucker flip occurred in residue C_{17} from the C3′-*endo* conformation to

(51) Thomson, J. B.; Tuschl, T.; Eckstein, F. *The Hammerhead Ribozyme*; Eckstein, F., Lilley, D. M. J., Eds.; Springer: New York, 1996; Vol. 10, pp 173−196.

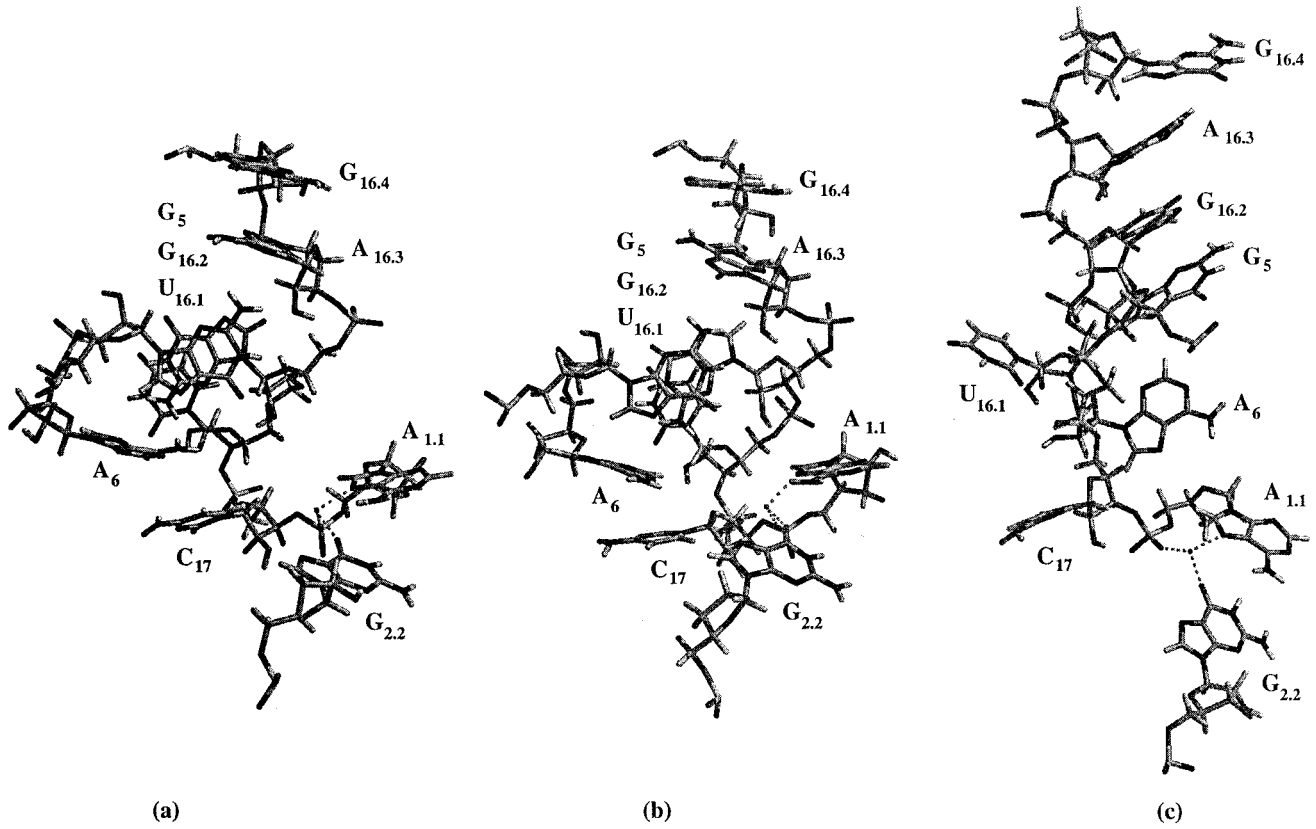

Figure 9. Comparison of NAC structures, showing the difference in stacking of the G_5, A_6, $U_{16.1}$, $G_{16.2}$, $A_{16.3}$, $G_{16.4}$, and C_{17} nucleotides between the first simulation, (a) and (b), and the replicate simulation (c) Structures (a), (b), and (c) are expanded views of Figures 4, 6, and 8, respectively. Although the stacking is different, NACs are spontaneously generated in both simulations.

the C2′-*endo* conformation. Following the structural rearrangements associated with effects **A** and **B**, NACs were subsequently generated. Figure 8 depicts a typical NAC structure from this simulation. In this simulation, it was also observed that a water molecule (wat2418) migrates into the active site. Wat2418 forms a hydrogen bond with the 2′-oxygen of residue C_{17} and with an inner sphere Mg^{2+} coordinated water. This hydrogen bonding pattern is somewhat different from that observed in the first simulation; however, it is consistent with the proposed mechanism for this reaction. A sugar pucker flip from the C2′-*endo* conformation back to the C3′-*endo* conformation occurred in residue C_{17} just prior to 900 ps of total simulation time. The C2′-*endo* conformation in C_{17} was not reestablished prior to the end of the replicate simulation. Also during equilibration, the nucleobases in the G_5-A_6-C_{17} platform became unstacked and remained unstacked for duration of the simulation. The nucleobase of residue C_{17} rotated out toward the major grooves while the nucleobase of residue A_6 rotated out toward the minor groove. The stacking platform of G_5-$G_{16.2}$-$U_{16.1}$ formed early in the equilibration period, but was quickly disrupted, as seen in the first simulation. Residues G_5 and $G_{16.2}$ then stacked with $A_{16.3}$ and $G_{16.4}$ of Stem II, while residue $U_{16.1}$ also rotated out toward the major groove and interacted with solvent. The base stacking differences here precluded hydrogen bonding interactions between A_6 and G_5 as well as that between A_6 and $G_{16.2}$ since the functional groups of these bases are not in close proximity to one another in this simulation. Unlike the first simulation, a persistent hydrogen bond between the *pro-R* oxygen of residue A_6 and the 2′-hydroxyl of residue G_5 formed, with an average distance of 2.13 ± 0.47 Å. Due to this persistent hydrogen bonding interaction, hydrogen bonds between residue G_5 and $C_{15.2}$, seen in the first simulation, did not form here. A persistent hydrogen bond between the *pro-R* oxygen of residue A_{13} and H21 of residue G_8 also occurred in this simulation; however, the average distance was slightly longer, 2.01 ± 0.27 Å compared with 1.86 ± 0.13 Å seen in the first simulation. The remaining exocyclic amine hydrogen of residue G_8 (H22) participated in two hydrogen bonding interactions with nearly identical distances to that seen in the first simulation. The average distance between H22 of G_8 and the O4′ of residue A_{13} was 2.58 ± 0.52 Å, while the distance between H22 of G_8 and N7 of A_{13} was 2.24 ± 0.23 Å. It is possible that the differences in base stacking (Figure 9) and hydrogen bonding patterns may be related to the number of NACs obtained in the replicate simulation.

Conclusions

Unconstrained molecular dynamics was used as a tool to supplement recent crystallographic data and provide mechanistically reasonable routes for the conformational changes necessary to go from the ground-state crystal structure to the transition state in the hammerhead ribozyme. The simulations suggest that the binding of the Mg^{2+} at the *pro-R* phosphate of residue $A_{1.1}$ induces conformational changes in the backbone of both strands at the active site, similar to that in ion-induced folding studies of the hammerhead ribozyme.[42,43,45,46] Conformational changes involving the conserved core residues, coupled with backbone rotations near the active site (effect **A**), and a sugar pucker flip from C3′-*endo* to C2′-*endo* in residue 17 (effect **B**) result in the positioning of the 2′-oxygen for an in-line attack on the phosphorus of the leaving nucleotide, residue 1.1. Thus, effects **A** and **B**, are shown to work in concert to generate near in-line attack conformations (Figures 4, 6, and 8) as originally proposed.[27] Reactive NACs formed approximately 18% of the

simulation time in the first study and 7% in the replicate simulation. Structural rearrangements from the X-ray crystal structure are accomplished and maintained through the interactions of the conserved nucleotide residues and the Mg^{2+} ions. One Mg^{2+} serves a purely structural role, while the other is ligated to the *pro-R* oxygen of the phosphodiester undergoing cleavage and thereby acts as a Lewis acid catalyst. In addition, this catalytic metal ion may function to neutralize the developing negative charge on the 5′-leaving group to facilitate its departure. The latter feature is evidenced by the motion of this Mg^{2+} toward the 5′-oxygen of residue $A_{1.1}$. The movements of the catalytic Mg^{2+} ion are consistent with the known mechanism of one-metal ion catalysis of phosphodiester hydrolysis[19] such that either a Mg^{2+}-ligated HO^- or a free HO^- can carry out the ionization to generate the nucleophile; however these results do not exclude additional mechanisms involving the participation of additional metal ions when near the active site.

Acknowledgment. This work was supported by a grant from the National Institutes of Health (DK09171) and a supplementary grant to R.A.T. from the National Institutes of Health. All computations were made possible by the National Science Foundation through the UCSB supercomputer grant (CDA96-01954) and Silicon Graphics Inc.

JA993094P